High-Content Screening and Profiling of Drug Activity in an Automated Centrosome-Duplication Assay

Zachary E. Perlman,*[a] Timothy J. Mitchison,[a] and Thomas U. Mayer*[b]

Maintenance of centrosome number is essential for cell-cycle progression and genomic stability, but investigation of this regulation has been limited by assay difficulty. We present a fully automated image-based centrosome-duplication assay that is accurate and robust enough for both careful cell-biology studies and high-throughput screening, and employ this assay in a series of chemical-genetic studies. We observe that a simple cytometric profiling strategy, which is based on organelle size, groups compounds with similar mechanisms of action; this suggests a simple strategy for excluding compounds that undesirably target such activities as protein synthesis and microtubule dynamics. Screening a library of compounds of known activity, we found unexpected effects on centrosome duplication by a number of drugs, most notably isoform-specific protein kinase C inhibitors and retinoic acid receptor agonists. From a 16320-member library of uncharacterized small molecules, we identified five potent centrosome-duplication inhibitors that do not target microtubule dynamics or protein synthesis. The analysis methodology reported here is directly relevant to studies of centrosome regulation in a variety of systems and is adaptable to a wide range of other biological problems.

Introduction

Centrosomes are the primary nucleators of microtubules in animal cells and play a number of essential signalling and structural roles in cell-cycle progression.[1] Abnormal numbers of centrosomes can result in abnormal mitotic spindle morphology, which may result in genomic instability. Consistent with this, abnormal centrosome numbers are observed in many types of cancer, and a growing body of evidence suggests that aneuploidy resulting from centrosome-duplication errors may play a causative role in tumour development, rather than simply being symptomatic.[2–6] Studies of centrosome regulation and the consequences of abnormal centrosome number have been slowed by the fact that centrosomes play regulatory roles throughout the cell cycle, thus complicating interpretation of genetic perturbations, and by the fact that conventional centrosome-counting assays are laborious and slow. We set out to identify new small-molecule reagents that might be used to block centrosome duplication with tight temporal control. To allow such a chemical genetic approach, we developed an automated assay that allows high-throughput counting of centrosome numbers in populations of cells.

Many cultured cell types, including Chinese hamster ovary (CHO) cells undergo multiple rounds of centrosome duplication when arrested in S-phase.[7] These overduplicated centrosomes often separate by a process whose molecular basis is unclear, allowing easy scoring of this phenomenon by light microscopy, and so this system has become a commonly used model for the study of centrosome regulation.[8–10] Routinely, S-phase arrests are imposed by treating tissue culture cells with hydroxyurea (HU), an inhibitor of ribonucleotide reductase, or with aphidicolin, an inhibitor of α-DNA polymerase. To ease analysis of centrosome overduplication and to allow high-throughput screening for pharmacological inhibitors, we adapted the conventional HU-arrest protocol[9] to a 384-well plate format. Trypsinized CHO cells were diluted into media containing 2 mM HU, dispensed in 384-well plates and treated with DMSO (control) or compounds. After 30 h of incubation, the cells were permeabilized, fixed and stained. Nuclei and centrosomes were labelled with Hoechst dye and anti-γ-tubulin antibodies, respectively; this allowed image acquisition by automated fluorescence microscopy.[11]

Since manual centrosome counting would be impossible for thousands of wells, we developed computational image-analysis algorithms to automate this task.[11] The assay requires the determination of centrosome number for every cell in an image, so we needed image segmentation methods that could reliably identify individual nuclei and γ-tubulin puncta associated with each nucleus. Since high-throughput staining and imaging conditions can lead to variations in image quality, we required algorithms that were robust to a range of cell densities and to nonuniform staining and illumination intensity. A Laplacian-based approach worked well for identifying discrete nuclei (see Experimental Section), and a standard top-hat filter served to identify centrosomes (Figure 1 A).[12] Counting the

[a] *Z. E. Perlman, Prof. T. J. Mitchison*
Department of Systems Biology and
Institute for Chemistry and Cell Biology, Harvard Medical School
Boston, MA 02115 (USA)
Fax: (+1) 617-432-5012
E-mail: zperlman@fas.harvard.edu

[b] *Dr. T. U. Mayer*
Max Planck Institute of Biochemistry
Chemical Biology, Independent Research Group
Am Klopferspitz 18, 82152 Martinsried (Germany)
Fax: (+49) 89-8578-3138
E-mail: mayer@biochem.mpg.de

 DOI: 10.1002/cbic.200400266

number of centrosomes associated with each nucleus generated population distributions for each image (Figure 1B) that were consistently within 5% of those obtained manually. Consistent with previous reports,[7] we observed that a substantial percentage of HU-arrested CHO cells contained more than two centrosomes (Figure 1A, control); this suggested that these cells had undergone multiple rounds of centrosome duplication. We note that the task of tallying discrete subcellular structures is one that arises across a broad class of biological problems, and our methodology can be adapted to many of these, including studies of aggresome formation,[13] chromosome missegregation[14] and multinuclearity due to cytokinesis failure.[15]

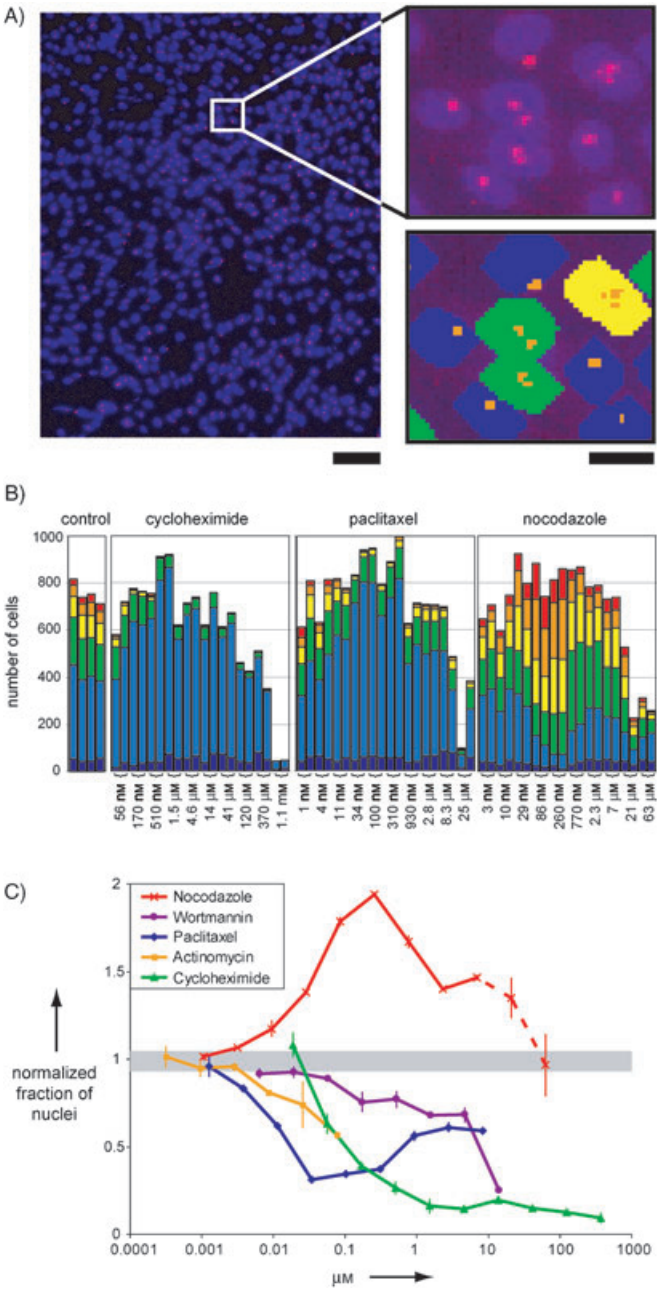

Figure 1. *An automated centrosome counting assay. A) Left, a typical fluorescence image; DNA shown in blue, γ-tubulin in red. Upper right, detail. Lower right, results of image processing; γ-tubulin shown in orange, nuclei containing 1 punctum in blue, 2 in green, 3 in yellow. Scale bars: 100 µm (left) and 20 µm (right). B) Stacked histograms showing dose-dependent changes in centrosome number distributions; colours as for (A) plus 0 punctum in dark blue, 4 in orange, >4 in red. C) Fraction of nuclei with 2 or more puncta (normalized to median of DMSO control population) as a function of drug dose. Points reflect averag of measurements performed in duplicate, with error bars extending to the original values. Those treatments giving >60% of the median number of cells from control populations are shown. For clarity, nocodazole wells with lower cell numbers are shown and indicated with a dotted line; we consistently observed the double peak seen here. Values are normalized by dividing by the median of the control populations. Grey region indicates 10th and 90th percentile values of control populations.*

We validated our assay by measuring centrosome numbers in cells treated with varying doses of compounds known to or likely to affect centrosome duplication or maturation.[9] Figure 1B shows the distributions observed with the microtubule depolymerizer nocodazole, the microtubule stabilizer paclitaxel or the protein-synthesis inhibitor cycloheximide. The stacked histograms shown reflect both the total number of cells and the distributions of numbers of discrete γ-tubulin puncta per nucleus (Figure 1B). To ensure consistency, we routinely tested each condition in duplicate. Although cell number varied slightly between wells treated under the same conditions, the distributions of centrosome numbers per cell remained remarkably consistent (Figure 1B). The decreased cell number at high concentrations of these compounds reflects cytotoxicity after 32 h of incubation (Figure 1B). However, at doses low enough to allow normal numbers of cells, the applied small molecules had a dramatic effect on the γ-tubulin punctum counts. Consistent with previous reports,[7] cycloheximide resulted in decreased apparent centrosome numbers over a wide range of doses. Paclitaxel, which has previously been reported to have little effect on centrosome duplication in CHO cells,[8] consistently decreased centrosome numbers under our assay conditions (Figure 1B). This difference could be due to the omission in our protocol of a compound washout prior to fixation. We speculate that the hyperstable microtubules generated by paclitaxel treatment increase aggregation of the replicated centrosomes and make it impossible to detect them as discrete objects. Most surprisingly, nocodazole consistently induced a dramatic increase in the number of cells with high apparent centrosome number (Figure 1B). We believe that this may reveal fragmentation of pericentriolar material or dispersal of multiple centrosomes as a result of microtubule depolymerization; this phenomenon is under more careful investigation by others.[16]

To reduce these data to a single measure for primary screening, we calculated the fraction of nuclei having two or more discrete centrosomes per nucleus and normalized this value by dividing by the median fractional value observed in control wells (Figure 1C). The dose-responsive changes in apparent centrosome numbers observed in Figure 1B are much more apparent in this analysis. This measure also makes clear that the fraction of the population having multiple centrosomes for a given treatment is remarkably consistent, even when the total number of cells varies significantly. In addition to the previously mentioned control compounds, we also observed dose-responsive reductions in centrosome numbers with two other compounds from the set we used for initial assay charac-

terization. These were the PI3 kinase inhibitor wortmannin and the DNA damager actinomycin, which inhibits transcription at higher doses (Figure 1C).

High-content image analysis can be further used to distinguish different mechanisms of perturbation. For example, both nuclei and centrosomes were distinctly dimmer and smaller in cycloheximide-treated cells, as might be expected upon general inhibition of protein synthesis (Figure 2A top). Similar results were seen with geldanamycin, an inhibitor of the chaperonin hsp90 previously reported to result in abnormal centrosome maturation and chromatin condensation,[17] although only at doses that also significantly lowered cell counts (data not shown). Morphological changes were induced by nocodazole and paclitaxel, but these are more subtle than would be easily noted by visual screening (Figure 2A bottom). To quantitate these changes, we determined the average area of the nuclear and centrosome regions generated for each image (Figure 2B). In this graph, each point represents the average of two measurements for a given concentration of drug, and the connecting line denotes the progression of a dosage series. This analysis made clear that compounds with different mechanisms of action have markedly different dose-dependent effects on area measures. For example, centrosomes were significantly smaller in nocodazole-treated cells (Figure 2B); this is consistent with pericentriolar fragmentation or decreased accumulation of pericentriolar material in the absence of the microtubule cytoskeleton. In contrast, paclitaxel treatment yielded cells with larger centrosomes (Figure 2B); this is consistent with previous observations[8] and suggests the possibility that this treatment inhibits separation or increases accumulation of pericentriolar material. Under these conditions, wortmannin yielded a dramatic increase in nuclear size over a wide range of doses, a phenomenon that has not yet been reported. These characteristic dose-dependent effects provide a kind of fingerprint for each of the compounds tested here, suggesting that even simple morphometric analysis can provide insight into compound activity and facilitate the grouping of compounds with similar molecular targets. Since these measures appeared to be very sensitive for detecting inhibitors of protein synthesis and of microtubule dynamics, we reasoned that such a strategy would facilitate the otherwise problematic task of discarding weak inhibitors of these processes.[18]

To validate this cytometric-profiling approach and to identify new processes involved in centrosome duplication, we screened an in-house set of 489 compounds for which targets had previously been reported.[19] We grouped compounds that affected centrosome number into categories suggested by the control analyses above (Table 1). Among the compounds that yielded nocodazole-like phenotypes were the three known microtubule depolymerizers in the test set, nocodazole, vinblastine and podophyllotoxin. Compounds that showed profiles similar to cycloheximide included the three protein-synthesis inhibitors in the set, anisomycin, cycloheximide and emetine, as well as camptothecin, a topoisomerase and transcription inhibitor.[20] The isoform-specific protein kinase C (PKC) inhibitor Gö6796 also matched this profile. PMA, a short-term PKC activator that down-regulates activity over long exposure,[21] also

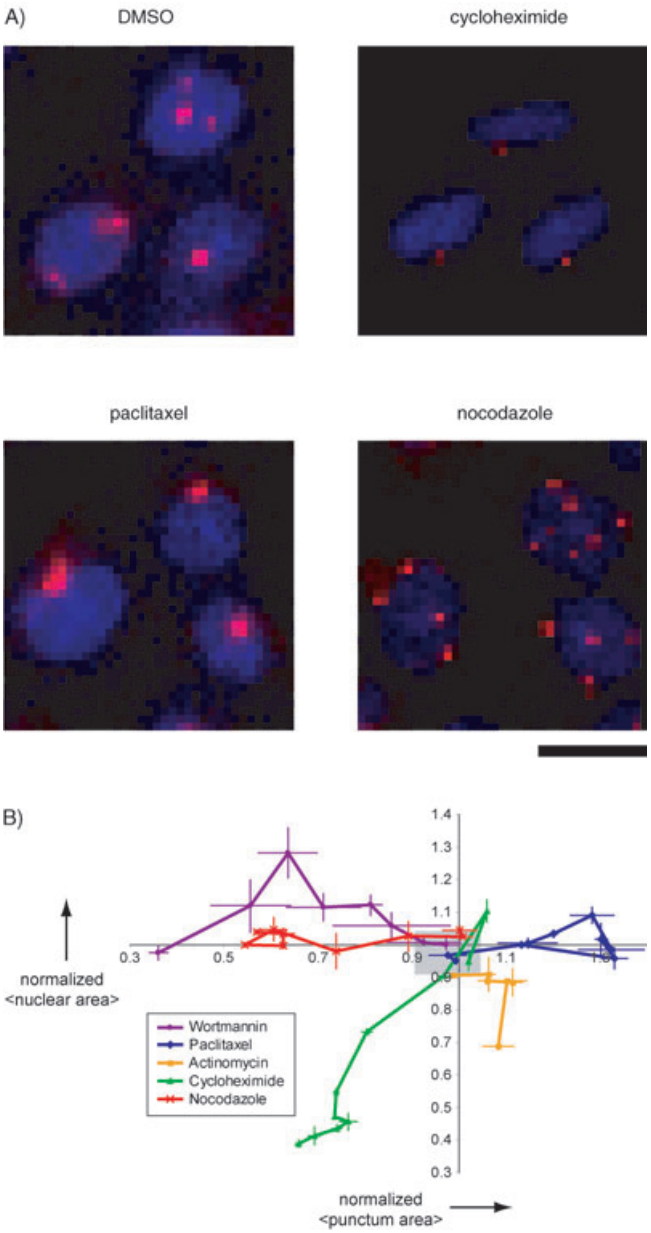

Figure 2. *Treatment of cells with different small molecules results in distinct changes in region size. A) Subtle differences are observable in nuclear and centrosome sizes in HU-arrested cells treated with 0.92 μM paclitaxel, 85 nM nocodazole or 370 μM cycloheximide; DNA shown in blue, γ-tubulin in red. Scale bar indicates 20 μm. B) Changes in region size are dose-dependent and correlated with different mechanisms of perturbing centrosome duplication. The points reflect the average of measurements performed in duplicate, with error bars extending to the original values. Values were normalized by dividing by the median of the control populations. Grey region indicates 10th and 90th percentile values of control populations.*

decreased centrosome numbers. Analysis of PKC in centrosome duplication is complicated by the fact that many PKC inhibitors cause apoptosis over long time periods.[22] Since PKC isoforms have been reported to localize to centrosomes during S-phase,[23,24] we consider it an open question whether PKC plays a functional role in centrosome duplication. Trichostatin, the only histone deacetylase inhibitor in the set, also reduced centrosome numbers. Recently, this class of drugs has been

Table 1. Known compounds[17] that affect centrosome counts at ~0.6 μg mL^{-1}, subdivided according to cytometric profile.

Decreased counts, smaller nuclei, smaller centrosomes—"cycloheximide-like"		Decreased counts, larger centrosomes—"taxol-like"		Increased counts, smaller centrosomes—"nocodazole-like"	
A-23187	Ca+ ionophore	cytochalasin D	actin depolymerizer	diphenylamine-iodonium	NADPH oxidase inhibitor
alsterpaullone	Cdk1/cdk5 inhibitor	Latrunculin B	actin depolymerizer	glutaraldehyde	cross-linker
anisomycin	translation inhibitor	SB202190	p38 MAP kinase inhibitor	nocodazole	microtubule depolymerizer
camptothecin	topo I/transcription inhibitor	taxol	microtubule stabilizer		
		PD 98059	MEK inhibitor		
cycloheximide	translation inhibitor				
		pifithrin	p53 inhibitor		
emetine	translation inhibitor				
		podophyllotoxin	microtubule depolymerizer		
Gö6796	PKC inhibitor			SKF-96365	Ca channel blocker
Gramicidin	H+/K+ ionophore			vinblastine	microtubule depolymerizer
menadione	oxidative stress, apoptosis inducer				
oligomycin A	F1 ATPase inhibitor	Decreased counts, no area change		Increased counts, no area change	
	antioxidative, ion channel	bafilomycin a1	13-*cis* retinoic	retinoic acid receptor agonist	
riluzole	blocker, PKC inhibitor	V-ATPase inhibitor			
staurosporine	broad-spectrum kinase inhibitor	curcumin	5-lipoxygenase, cyclo-oxygenase inhibitor	9-*cis* retinoic acid	retinoic acid receptor agonist
monensin	Na+ ionophore	diethylnorspermine (*N*,*N*)	polyamine biosynthesis	forskolin	cAMP increaser
FCCP	H+ ionophore	phorbol 12 myristate 13 acetate	PKC activator/long-term inhibitor	retinoic acid, all *trans*	retinoic acid receptor agonist
Leptomycin	nuclear export inhibitor	TPEN	divalent cation chelator		
valinomycin	K+ ionophore	trichostatin-A	HDAC inhibitor		

shown to reduce dynein-dependent transport to the centrosome;[25] this confirms the hypothesis that PCM-1 or other centrosomal components have to be targeted to the centrosome in order to allow centrosome duplication.[8] Three retinoic acid isomers and the adenylate cyclase activator forskolin reproducibly increased centrosome counts without affecting centrosome area. Retinoic acid is known to promote cAMP-dependent cell growth and differentiation in a number of cell types,[26] and our results suggest that this signalling might also be important for centrosome regulation. These results show that this simple profiling approach can group compounds that affect common pathways, can allow the exclusion from further analysis of compounds affecting undesired targets, and can also suggest new centrosome biology.

High-throughput phenotypic screening of small-molecule libraries can identify new therapeutic lead compounds and reveal new proteins involved in processes of interest. We used our profiling approach to screen for centrosome-duplication inhibitors that do not inhibit microtubules or protein synthesis. We screened a 16320-member library of small molecules for inhibitors of centrosome duplication and identified 35 compounds that at 10 μM reproducibly changed the percentage of cells containing multiple γ-tubulin puncta (Figure 3A). Subsequent experiments identified 15 compounds with inhibitory activity at or below 1 μM. Eleven of these potent inhibitors showed cytometric profiles similar to those of the protein-synthesis inhibitor, microtubule depolymerizer and microtubule stabilizer control compounds in Figure 2B. In vitro microtubule depolymerization assays are relatively insensitive, and we have had recurring problems excluding weak depolymerizers in other assays, so we discarded the five compounds matching the nocodazole-profile. We also discarded the three members of the protein-synthesis-inhibitor profile, and further tested this approach by confirming that no remaining compounds inhibited in an in vitro transcription assay and an assay of incorporation of ^{35}S-methionine by cultured cells (data not shown). We performed a combination of FACS analysis and comparison against other screens previously performed at the Harvard Institute for Chemistry and Cell Biology (ICCB) to identify cell-cycle inhibitors from the three compounds that matched the paclitaxel profile and the four compounds that did not match any of these profiles (Figure 3B, CDIs 1–4). One of the three paclitaxel-like compounds did not affect cell-cycle progression; this suggests that it decreases apparent centrosome numbers while increasing area by a mechanism other than microtubule stabilization (Figure 3B, CDI 5). We speculate that this compound might act on microtubule-associated motors or upstream signalling pathways. To confirm that CDIs 1–5 affect centrosome duplication rather than the distribution of γ-tubulin, we treated HU-arrested CHO cells with 25 μM of CDIs 1–5 and confirmed that the distribution of pericentrin, an integral component of the pericentriolar material, was the same as that of γ-tubulin (Figure 3C). We have thus identified five compounds that are likely to inhibit the centrosome maturation process by new mechanisms, and we are working to identify their protein targets.

Investigations of centrosome duplication and of the hypothesis that misregulated duplication plays a role in tumourigenesis[2–6] have been hindered by the fact that manual scoring of centrosome counts is slow and laborious. The establishment of

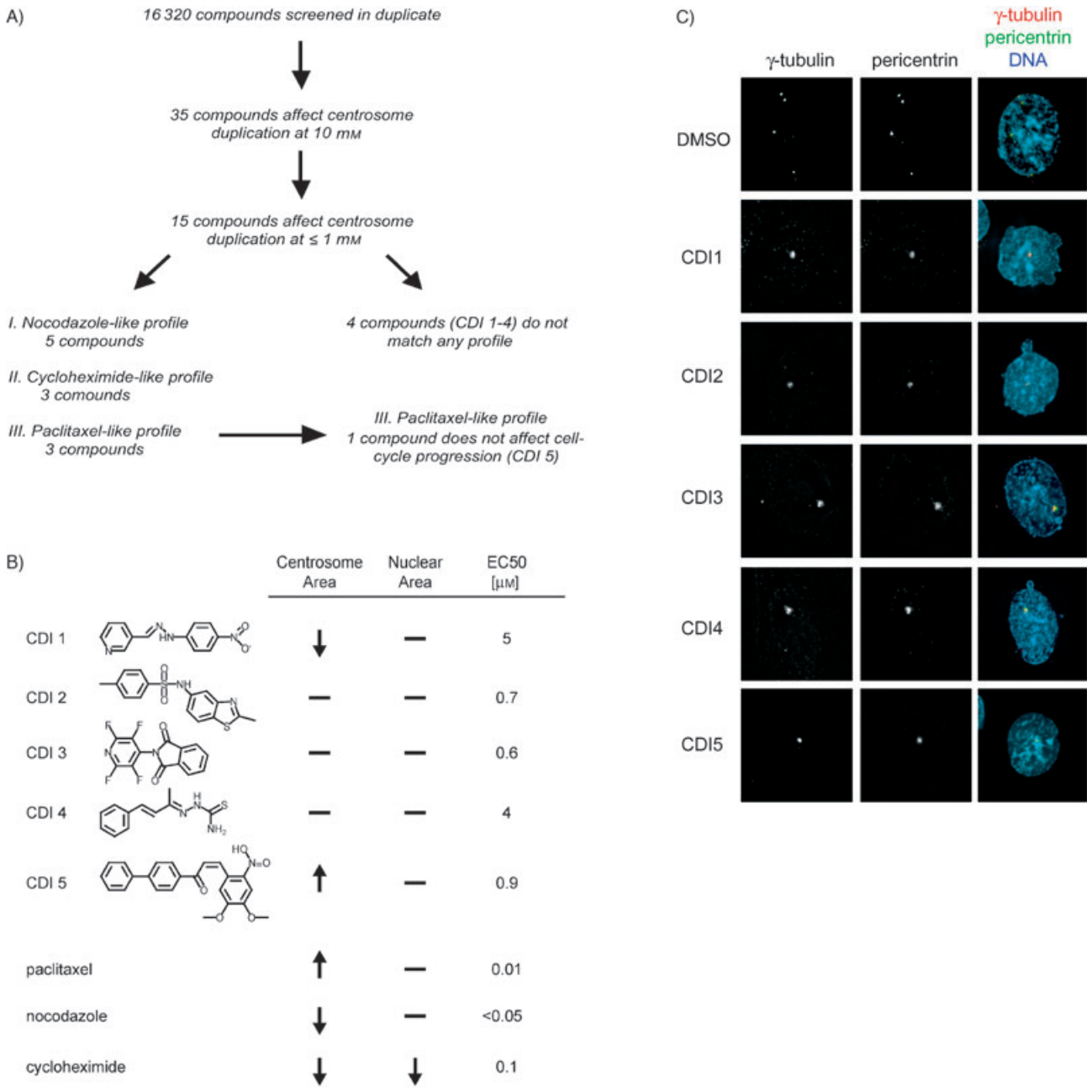

Figure 3. *Five compounds inhibit centrosome overduplication in HU-treated CHO cells through different mechanisms than the drugs shown in Figure 2B. A) Scheme of the screening results for potent inhibitors of centrosome duplication. B) Structures of centrosome-duplication inhibitors CDI 1–5. Arrows indicate the effect on the centrosome and nuclear area at the EC_{50}. EC_{50}s were obtained by interpolating between the two values flanking the half-maximal change in apparent centrosome count. C) Immunofluorescence images of HU-arrested CHO cells treated with 25 μM CDI 1–5.*

high-throughput methods is thus a necessary step towards comprehensive studies of this biology. Centrosome overduplication has been shown to occur upon HU arrest in human cell lines,[27] and it should be straightforward to extend our methodology to such other cell types. We note that mechanistic understanding of the effects of compounds that score in this assay will require significant further cell biological characterization. Although this assay is routinely presumed to reflect normal centrosome-maturation processes, it is difficult, without electron microscopy, to distinguish real centrosome duplication from changes in apparent number due to defects in centriole separation or integrity of the pericentriolar matrix.

Although we have focused on high-throughput screening and analysis of small molecule inhibitors, our methods are equally suitable for genetic screening and quantitative investigations of large sets of perturbations, and potentially could be used to analyze tissue or clinical samples. The automated counting algorithm is robust and versatile, and has already been adapted to other analysis-limited assays such as fluorescence in situ hybridization, aggresome counting and identifica-

tion of multinucleate cells.[13–15] The screening and image-analysis methodology we outline here should thus be useful in basic cell biology, drug discovery and more clinical contexts.

Our results also show that high-throughput microscopy and computational image analysis remain underexploited tools for mechanistic analysis of cell phenotypes. First, the observation that relatively small changes in organelle size can be reproducibly measured suggests that it is possible to assess more subtle phenotypes than have conventionally been addressed in cell biology. Second, although high-content screening by microscopy has been used to weed out toxic compounds,[28] and profiling by using the joined results of multiple image-based screens has been reported,[29] our results hint that clustering with even a small number of cytometric measures from a single screen may provide mechanistic insight by grouping perturbations of similar basis, an idea we have begun to develop further.[30]

Experimental Section

Cell culture and immunofluorescence. CHO cells in McCoy's 5A media (Invitrogen/GIBCO, Carlsbad, CA) supplemented with 10% foetal calf serum and 10 mM HEPES, pH 7.4, were plated into tissue culture-treated clear-bottom 384-well plates (Nalge Nunc International, Rochester, NY) at a density of 7000 cells per well, final volume 30 μL. The plates were spun for 1 min at 1000 rpm in a tabletop centrifuge and incubated overnight at 37 °C, 5% CO_2. HU stock in media (10 μL, 8 mM) was added, compound stocks in DMSO (100 nL) were transferred by using a robot-controlled stainless-steel pin array,[31] resulting in a 400-fold dilution, and plates were returned to the incubator for 32 h.

To prepare cells for immunofluorescence, media were aspirated and replaced with PBS (50 μL), pH 7.2, which was immediately replaced with two exchanges of perm buffer (50 μL; 100 mM K-Pipes, 10 mM EGTA, 1 mM $MgCl_2$, 0.2% Triton-X 100). After 5 min, this was aspirated and replaced with methanol at −20 °C, taking care to maintain cold temperature. Plates were incubated at −20 °C for 10 min, then washed twice with TBS-TX buffer (10 mM Tris, pH 7.5, 100 mM NaCl, 0.1% Triton-X 100), followed by 2 h incubation in AbDil (50 μL; TBS-TX-100, 2% BSA). Cells were then incubated for 1 h in anti-γ-tubulin (20 μL, 1:1000, Sigma) in AbDil, washed with TBS-TX (2×50 μL) and AbDil (1×50 μL). Alexa-594 goat anti-mouse secondary antibody (20 μL, 1:250 dilution, Molecular Probes) and Hoechst 33342 (1 μg mL^{-1}, Sigma) in AbDil was applied for 1 h, followed by washing with TBS-TX-100 (2×50 μL). For high-throughput screening, all liquids were dispensed by using an eight-channel Multidrop (Labsystems). For follow-up imaging, cells were treated as above, with the addition of anti-pericentrin antibody (gift from Christiane Wiese) during the primary incubation and Alexa-488 goat anti-rabbit antibody (Molecular Probes) during the secondary incubation.

Compound libraries. High-throughput screening was performed on a 16320-member library of uncharacterized compounds (Diverse E set, Chembridge Corp.; plated in 10 mM stock solutions in DMSO), a 489-member of known bioactive compounds prepared at ICCB (plated at 5 mg mL^{-1}, 1.1 mg mL^{-1} and 0.25 mg mL^{-1} in DMSO), and a 1040-member library provided by the National Institutes of Neurological Disease and Stroke (plated at 10 mM in DMSO). All plates were screened in duplicate. The compounds used for initial assay calibration plates and compounds reordered after primary screening were dissolved in DMSO and prepared in threefold dilution series ranging from 5 to 10 mM.

Image acquisition. High-throughput screening images were acquired by using a NikonTE300 inverted fluorescence microscope equipped with an automated filter wheel (Sutter), motorized *x*–*y* stage (Prior), piezoelectric-motorized objective holder (Physik Instrumente), cooled CCD camera (Hamamatsu) and a robotic plate-transfer crane (Hudson) all controlled by Metamorph software (Universal Imaging). A Plan Fluor 10× objective was used with 2×2 binning on chip. Acquisition required ~1 h per plate. Follow-up images were acquired as *z*-series by using a Nikon TE200 microscope with a 60× Plan Fluor objective, and were deconvolved by using Deltavision software and displayed as projections.

Image analysis. Images were analyzed with software custom-written by using Visual Basic 6.0 (Microsoft) and Halcon 6.0.1 (MVTec Software). This software iterates the algorithm over all images specified by the HTS parameter files produced by Metamorph and returns the resulting values to an Excel spreadsheet. Analysis required an average of 4 s on a typical PC for an image containing 600–1000 cells.

Nuclear region segmentation. To maximize robustness to variation in staining and illumination intensity, as well as to minimize the need for assumptions about nuclear size and shape, we used a rapid-segmentation approach that relies solely on the sign of the second derivative of fluorescence intensity. In contrast to the more conventional use of zero-crossings in the second derivative as part of an edge-detection strategy, we took advantage of the convexity of nuclear intensity at low resolutions and directly identified discrete regions of negative-valued Laplacian; we have recently described this approach elsewhere.[30] DAPI intensity images were convolved with a Laplacian-of-a-Gaussian kernel[12] of width 1.75 pixels, and values less than −1 were identified in this filtered image. Holes in the resulting regions were filled, and following a morphological erosion with a disc of radius 2 pixels, discrete regions falling within a size range specified manually for each plate were identified. Following dilation by a disc of radius 4 pixels, these regions were identified as nuclear regions.

Centrosome-region segmentation. To identify centrosomes while excluding larger debris in the γ-tubulin staining, we applied a top-hat filter whose inner and outer radii were set manually for each plate and then identified for values above a manually determined value.[12]

Measures. The number of discrete regions in the intersection of the set of centrosome regions with each nuclear region is defined as the centrosome count for that nuclear region. For each image, the number of nuclear regions with centrosome counts of 0, 1, 2, 3, 4 or >4 was recorded. The mean area for each plate of the nuclear regions and of the centrosome regions was recorded.

Data analysis. We frequently observed row-to-row variation in staining intensity, which we attributed to systematic high-throughput liquid-handling errors. As such, all high-throughput screening values were normalized by dividing by the median value for each row. For known-compound and screening follow-up plates, measurements were divided by the median value of DMSO control wells placed at multiple positions on the plate. To select high-throughput screening compounds for follow-up, Excel macros were used to identify wells for which the mean value of experimental replicates scored >2 standard deviations from the norm, with the added restriction that the difference between the two replicate values had to be less than a manually set threshold.

Acknowledgements

We thank Yan Feng, Jon Hoyt, Justin Yarrow and the ICCB screening room staff for technical expertise and instrument maintenance. We thank Paul Chang, Stefan Hümmer and Ann Yonetani for comments on the manuscript. Z.E.P. is an HHMI Predoctoral Fellow. T.U.M. is supported by an Emmy Noether Fellowship of the DFG. This work was supported by grants from the NIH (CA78048), and Merck & Co., Europe.

Keywords: bioinformatics · biological information · centrosomes · drugs · high-throughput screening

[1] C. L. Rieder, S. Faruki, A. Khodjakov, *Trends Cell Biol.* **2001**, *11*, 413.
[2] A. B. D'Assoro, W. L. Lingle, J. L. Salisbury, *Oncogene* **2002**, *21*, 6146.
[3] S. Doxsey, *Mol. Cell* **2002**, *10*, 439.
[4] S. Duensing, K. Munger, *Crit. Rev. Eukaryotic Gene Expression* **2003**, *13*, 9.
[5] E. A. Nigg, *Nat. Rev. Cancer* **2002**, *2*, 815.
[6] G. Sluder, J. J. Nordberg, *Curr. Opin. Cell Biol.* **2004**, *16*, 49.
[7] R. Balczon, L. Bao, W. E. Zimmer, K. Brown, R. P. Zinkowski, B. R. Brinkley, *J. Cell Biol.* **1995**, *130*, 105.
[8] R. Balczon, C. E. Varden, T. A. Schroer, *Cell Motil. Cytoskeleton* **1999**, *42*, 60.
[9] R. Balczon, *Methods Cell Biol.* **2001**, *67*, 257.
[10] A. Khodjakov, C. L. Rieder, G. Sluder, G. Cassels, O. Sibon, C. L. Wang, *J. Cell Biol.* **2002**, *158*, 1171.
[11] J. C. Yarrow, Y. Feng, Z. E. Perlman, T. Kirchhausen, T. J. Mitchison, *Comb. Chem. High Throughput Screening* **2003**, *6*, 279.
[12] J. C. Russ, *The Image Processing Handbook*, 4th ed., CRC Press, Boca Raton, FL, **2002**.
[13] Q. Liu, Z. E. Perlman, T. J. Mitchison, unpublished results
[14] Q. Shi, Z. E. Perlman, R. King, unpublished results
[15] U. S. Eggert, A. A. Kiger, C. Richter, Z. E. Perlman, N. Perrimon, T. J. Mitchison, C. M. Field, *PLoS Biol.* **2004**, *2*, E379.
[16] E. S. Halpin, E. H. Hinchcliffe, *Mol. Biol. Cell* **2003**, *14*, 1842.
[17] B. M. Lange, A. Bachi, M. Wilm, C. Gonzalez, *EMBO J.* **2000**, *19*, 1252.
[18] S. J. Haggarty, T. U. Mayer, D. T. Miyamoto, R. Fathi, R. W. King, T. J. Mitchison, S. L. Schreiber, *Chem. Biol.* **2000**, *7*, 275.
[19] http://iccb.med.harvard.edu/screening/compound_libraries/bioactives iccb_1.html
[20] C. J. Thomas, N. J. Rahier, S. M. Hecht, *Bioorg. Med. Chem.* **2004**, *12*, 1585.
[21] J. R. Hepler, H. S. Earp, T. K. Harden, *J. Biol. Chem.* **1988**, *263*, 7610.
[22] J. S. Liou, J. S. Chen, D. V. Faller, *J. Cell. Physiol.* **2004**, *198*, 277.
[23] D. Chen, A. Purohit, E. Halilovic, S. J. Doxsey, A. C. Newton, *J. Biol. Chem.* **2004**, *279*, 4829.
[24] M. Passalacqua, M. Patrone, B. Sparatore, E. Melloni, S. Pontremoli, *Biochem. J.* **1999**, *337 (Pt 1)*, 113.
[25] L. J. Corcoran, T. J. Mitchison, Q. Liu, *Curr. Biol.* **2004**, *14*, 488.
[26] M. B. Sporn, A. B. Roberts, D. S. Goodman, *The Retinoids: Biology, Chemistry, and Medicine*, 2nd ed., Raven, New York, **1994**.
[27] V. M. Stucke, H. H. Sillje, L. Arnaud, E. A. Nigg, *EMBO J.* **2002**, *21*, 1723.
[28] J. H. Price, A. Goodacre, K. Hahn, L. Hodgson, E. A. Hunter, S. Krajewski, R. F. Murphy, A. Rabinovich, J. C. Reed, S. Heynen, *J. Cell Biochem. (Supplement)* **2002**, *39*, 194.
[29] V. C. Abraham, D. L. Taylor, J. R. Haskins, *Trends Biotechnol.* **2004**, *22*, 15.
[30] Z. E. Perlman, M. Slack, Y. Feng, T. J. Mitchison, L. Wu, S. Altshuler, *Science*, **2004**, *306*, 1194 – 1198
[31] L. A. alling, N. R. Peters, E. J. Horn, R. W. King, *J. Cell Biochem. (Supplement)* **2001**, *37*, 7.

Received: July 27, 2004
Early View Article
Published online on November 29, 2004

